Combined T_1 and T_2 Measurement for Non-Invasive Evaluation of Blood Oxygen Saturation and Hematocrit

Sharon Portnoy[1], Mike Seed[2], Julia Zhu[2], John G. Sled[1,3], and Christopher K. Macgowan[1,4]

[1]*Department of Medical Biophysics, University of Toronto, Toronto, Ontario, Canada,* [2]*Diagnostic Imaging, The Hospital for Sick Children, University of Toronto, Toronto, Ontario, Canada,* [3]*Mouse Imaging Centre, The Hospital for Sick Children, Toronto, Ontario, Canada,* [4]*Diagnostic Imaging, The Hospital for Sick Children, Toronto, Ontario, Canada*

Purpose: MRI properties of whole blood (i.e. plasma + erythrocytes) are a function of both hematocrit, *Hct*, and oxygen saturation, sO_2. Vascular MR oximetry measurements typically compute sO_2 only, while assuming a normal value for *Hct* (0.45). Although this assumption may be valid in healthy adults, it might not apply to diseased patients or to our population of interest: fetuses potentially affected by hypoxia. An increase in *Hct* is a known adaptation of the fetus to chronic hypoxia. In cases of maternal alloimmunization, fetal *Hct* may be reduced. Accordingly, our objective is to establish whether a combination of vascular T_1 and T_2 measurements can be reliably used to determine both sO_2 and *Hct*, facilitating a more accurate and complete hematological assessment.

Methods:

Sample Preparation: Human blood was obtained from adult volunteers. The blood was divided into 14 samples (placed in vacutainer tubes) which were processed to provide a range of *Hct* and sO_2. *Hct* was adjusted by removal/addition of separated plasma. sO_2 was lowered by exposure to nitrogen gas.

MRI Acquisition: Samples were scanned at room temperature on a 3T system (Siemens TRIO). T_2 relaxation times were measured using a multi spin echo sequence with 32 echoes and a 12.2 ms echo spacing (6.5min scan duration). T_1 relaxation times were measured using a Modified Look Locker Inversion Recovery (MOLLI) pulse sequence with 15 inversion times, *TI*, from 100 to 8135 ms (4min scan duration). To minimize erythrocyte settling, blood samples were agitated prior to each scan. Sample preparation and MRI scanning were performed within 48 hours of blood drawing. When not being processed/scanned, blood samples were stored at 4°C.

Blood Gas Analysis: Immediately following MRI, sample hematocrit and oxygen saturation were measured using an ABL800 FLEX Blood Gas Analyzer (Radiometer, Copenhagen, Denmark). Sample manipulations resulted in a range of 0.2-0.54 for *Hct* and 0.1-1.0 for sO_2.

Data Processing:

- Regions of interest were manually drawn in each sample tube. For each sample, T_2 was obtained from a mono-exponential fit of the mean spin-echo ROI signal. T_1 was evaluated by fitting the ROI signal at each inversion time to the three-parameter exponential: $S=A+B\cdot exp(-TI/T_1^*)$. As is typical for Look-Locker data, the apparent relaxation time, T_1^*, was then used to compute the "corrected" T_1: $T_1=T_1^*(B/A-1)$ [1].
- $R_2=T_2^{-1}$ data for all samples were then fit to the following relationship [2], which is based on a two-compartment exchange model for blood [3]: $R_2=A+B\cdot(1-sO_2)+C\cdot(1-sO_2)^2$. Coefficients *A*, *B* and *C* depend on *Hct*: $A=a_1+a_2\cdot Hct+a_3\cdot Hct^2$, $B=b_1\cdot Hct+b_2\cdot Hct^2$, $C=c_1\cdot Hct\cdot(1-Hct)$. The six coefficients, a_1, a_2, a_3, b_1, b_2, and c_1, which are obtained from the fit, depend on various physical and experimental parameters, such as the frequency difference between oxy- and deoxyhemoglobin, the rate of spin exchange between plasma and erythrocytes, and the pulse sequence echo spacing.
- $R_1=T_1^{-1}$ data was fit to the relationship: $R_1=Hct\cdot R_{1,ery}+(1-Hct)\cdot R_{1,plas}$, where $R_{1,ery}$ and $R_{1,plas}$ refer to the relaxation rates of erythrocytes and plasma. Since deoxyhemoglobin behaves as a weak, paramagnetic contrast agent [4], $R_{1,ery}$ is, in turn, dependent on oxygen saturation: $R_{1,ery}=R_{1,ery}\cdot(sO_2=1)+Q\cdot(1-sO_2)$. The fit to R_1 data yields 3 parameters: $R_{1,ery}(sO_2=1)$, $R_{1,plas}$, and *Q*.

*Table 1: Summary of model parameters from R_1/R_2 data fits. Uncertainties refer to the 68% confidence bounds. *In the R_2 fit, coefficients a_2 and a_3 were set to 0, since the chi-squared of the fit was not sensitive to these parameters.*

Parameter	a_1 [s^{-1}]	a_2 [s^{-1}]	a_3 [s^{-1}]	b_1 [s^{-1}]	b_2 [s^{-1}]	c_1 [s^{-1}]	$R_{1,plas}$ [s^{-1}]	$R_{1,ery}(sO_2=1)$ [s^{-1}]	*Q*
Value	6.14 ± 0.49	0*	0*	-95 ± 25	175 ± 39	239 ± 38	0.54 ± 0.02	0.93 ± 0.05	0.27±0.06

Results: Parameters from fits to R_1 and R_2 data are summarized in Table 1. Fitted functions $R_1(Hct,sO_2)$ and $R_2(Hct,sO_2)$ constitute a system of two equations, which can be inverted to obtain expressions for $Hct(R_1, R_2)$ and $sO_2(R_1,R_2)$. $Hct(R_1,R_2)$ and $sO_2(R_1,R_2)$ are the roots of a cubic polynomial, which, depending on the values of R_1 and R_2, can have up to 3 real solutions for *Hct* and sO_2. The feasibility of evaluating *Hct* and sO_2 from a pair of R_1/R_2 measurements hinges on the presence of a single, physical (i.e. $0\leq Hct\leq 1$ and $0\leq sO_2\leq 1$) solution for the specific R_1/R_2 combination. Solutions for $Hct(R_1,R_2)$ and $sO_2(R_1,R_2)$ are plotted in Figure 1.

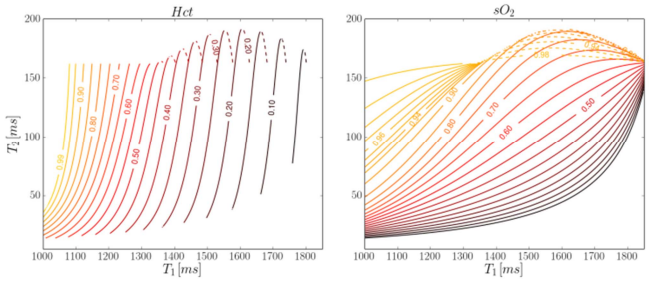

Figure 1: Contour plots of $Hct(T_1,T_2)$ and $sO_2(T_1,T_2)$. Note the region of overlap between two solutions (as indicated by solid and dashed contour lines) in the upper right quadrant.

To test the accuracy of the solutions, measured R_1/R_2 values were used to calculate the underlying *Hct* and sO_2. Calculated values were then compared to the true *Hct* and sO_2 obtained from blood gas analysis (see Fig. 2). A Monte-Carlo technique was used to establish how error in R_1/R_2 estimation propagates through to *Hct* and sO_2 evaluation. Specifically, each calculation was repeated 10000 times, with R_1/R_2 values obtained from a normal distribution with a mean equal to the actual R_1/R_2 estimate and standard deviation equal to the R_1/R_2 uncertainty (determined from the 68% confidence interval of the fit). In general, correspondence between calculated and true values of *Hct* and sO_2 is good. On average, the relative accuracy ($RA=|calc-true|/true$) was 8% for *Hct* and 30% for sO_2.

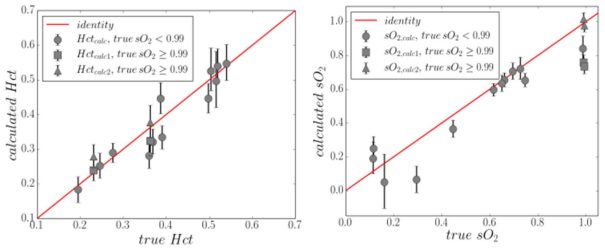

Figure 2: Correspondence between calculated/true values of Hct/sO_2. For samples with true $sO_2\geq 0.99$, there are 2 calculated Hct/sO_2 values. Errorbars represent the interquartile range from the distribution of $Hct_{calc}/SO_{2,calc}$ obtained from 10000 Monte-Carlo selections of R_1/R_2.

Discussion: For the majority of T_1/T_2 combinations the condition of a single, physical solution is fulfilled. However, in the upper right quadrant of Fig. 1 (T_1>1300 ms, T_2>160 ms) there is a region of overlap between two solutions. For T_1/T_2 pairs within this range, there are two possible combinations of *Hct* and sO_2 . In one of the combinations, sO_2 will be very high (~1.0). This solution can generally be ruled out in a fetal population, where blood $sO_2\leq 0.85$, even under normoxic conditions [5]. Note that the issue of two possible solutions would similarly arise in the case of an assumed hematocrit, Hct_0, and a single T_2 estimate. In this case, $sO_2(Hct_0, T_2)$ is the solution to a quadratic polynomial, which, if T_2>160 ms, has 2 real, physical roots. While the limited accuracy of sO_2 estimates (30%, on average) may be concerning, it is an improvement upon what would be obtained with a single T_2 measurement and an assumed *Hct* of 0.45 (45% relative accuracy, on average).

Conclusion: Combining T_1 and T_2 measurements improves the accuracy of sO_2 estimation and provides a reliable means of evaluating *Hct*. This is particularly helpful in a fetal population, as it provides a non-invasive alternative to cordocentesis for determining blood oxygen saturation and hematocrit.

References: [1] Deichmann R, Haase A. *J Magn Reson.* 1992, 96:608-612. [2] Lu H, *et al*. *Magn Reson Med.* 2012; 67:42-49. [3] Luz Z, Meiboom S. *J Chem Phys.* 1963; 39(2):366. [4] Grgac K, *et al*. *Magn Reson Med.* 2013; 70:1153-1159. [5] A. Rudolph. *Congenital Diseases of the Heart.*Wiley, 2011.